Thermal Isolation of Encapsulated MEMS Resonators

Chandra Mohan Jha, *Student Member, ASME*, Matthew A. Hopcroft, Saurabh A. Chandorkar, James C. Salvia, *Student Member, IEEE*, Manu Agarwal, *Member, IEEE*, Rob N. Candler, *Member, IEEE*, Renata Melamud, Bongsang Kim, and Thomas W. Kenny

***Abstract*—This paper presents an in-chip thermal-isolation technique for a micro-ovenized microelectromechanical-system resonator. Resonators with a microoven can be used for high-precision feedback control of temperature to compensate for the temperature dependence of resonator frequency over a wide temperature range. However, ovenization requires power consumption for heating, and the thermal time constant must be minimized for effective temperature control. This paper demonstrates an efficient local-thermal-isolation mechanism, which can reduce the power requirement to a few milliwatts and the thermal time constant to a few milliseconds. In this method, the mechanical suspension of the resonator is modified to provide thermal isolation and include an integrated resistive heater. This combination provides mechanical suspension, electrical heating, and thermal isolation in a compact structure that requires low heating power and has a small thermal time constant. A power consumption of approximately 12 mW for a 125 °C temperature rise and a thermal time constant ranging from 7 to 10 ms is reported in this paper, which is orders of magnitude lower than that of commercially available ovenized quartz resonators. A CMOS-compatible wafer-scale encapsulation process is used to fabricate this device, and the thermal-isolation design is achieved without any modification to the existing resonator fabrication process. [2007-0042]**

***Index Terms*—Encapsulation, microelectromechanical devices, microresonators, thermal isolation.**

NOMENCLATURE

k	Thermal conductivity, W m^{-1} K^{-1}.
ε	Surface emissivity, $0 \leq \varepsilon \leq 1$.
σ	Stefan–Boltzmann constant, 5.67×10^{-8}W m^{-2}K^{-4}.
ρ	Density, kg m^{-3}.
c_p	Specific heat capacity at constant pressure, J kg^{-1} K^{-1}.
R_e	Electrical resistance, Ω.
$R_{\rm th}$	Thermal resistance, K W^{-1}.
C	Specific heat per unit volume at constant volume, J m^{-3} K^{-1}.
ν	Velocity of the energy carrier, m s^{-1}.
k_B	Boltzmann constant, 1.381×10^{-23} J K^{-1}.
n_m	Molecular number density, m^{-3}.
m	Molecular mass of the energy carrier, kg.
T	Temperature, K.
V'	Volume, m^3.
V	Voltage, V.
$C_{\rm chip}$	Thermal capacitance of chip, J K^{-1}.
$C_{\rm resonator}$	Thermal capacitance of resonator, J K^{-1}.
A_c	Cross-sectional area, m^2.
A_s	Surface area, m^2.
q'	Rate of joule heat per unit volume, W m^{-3}.
q	Rate of total heat generated, W.
l	Length, m.
E	Modulus of elasticity, N m^{-2}.
I	Area moment of inertia, m^4.
P	Axial force, N.
m_l	Mass per unit length, kg m^{-1}.
f	Frequency, Hz.

Manuscript received February 21, 2007; revised June 10, 2007. This work was supported in part by DARPA HERMIT under Grant ONRN66001-03-1-8942, in part by the Robert Bosch Corporation, Palo Alto Research and Technology Center, in part by a CIS Seed Grant, in part by The National Nanofabrication Users Network facilities funded by the National Science Foundation under Award ECS-9731294, and in part by The National Science Foundation Instrumentation for Materials Research Program under Grant DMR 9504099. Subject Editor D. DeVoe.

C. M. Jha, M. A. Hopcroft, S. A. Chandorkar, J. C. Salvia, M. Agarwal, R. Melamud, B. Kim, and T. W. Kenny are with the Department of Mechanical and Electrical Engineering, Stanford University, Stanford, CA 94305 USA (e-mail: cmjha@stanford.edu).

R. N. Candler was with Stanford University, Stanford, CA 94305 USA. He is now with the Robert Bosch Corporation Research and Technology Center, Palo Alto, CA 94304 USA.

Color versions of one or more of the figures in this paper are available online at http://ieeexplore.ieee.org.

Digital Object Identifier 10.1109/JMEMS.2007.904332

I. INTRODUCTION

THE CMOS-compatible microelectromechanical-system (MEMS) resonators are becoming an interesting and viable technology [1]–[7] as a replacement for quartz crystals [8]–[13] for timing- and frequency-reference applications. Currently, oven-controlled quartz resonators are used to generate high-precision frequency references suitable for high-end industry and military standards [10]–[13]. In this method, the resonator is held at a fixed temperature to compensate for the temperature dependence of the resonator frequency. The extent to which the resonator is heated depends on the difference between the set point and the ambient temperature. For an ovenized resonator that is required to operate within a temperature range of -40 °C to 85 °C, the heating has to cover a range of 125 °C. Due to the large volume of a conventional quartz-crystal oscillators, which can be up to 1000 mm^3 [14], the power consumption for heating can be as much as 10 W with a warm-up time of approximately 30 min [13]–[15]. MEMS technology offers miniaturization to submillimeter scales, which can provide substantial power reduction [1], [16]–[18].

A microoven, in general, constitutes a heater for joule heating and thermal isolation for reducing heat loss. Microoven designs for MEMS devices have been reported with few milliwatts of power consumption and a time constant in milliseconds [16]–[18]. In these designs, a MEMS structure is suspended on a microplatform. The microplatform is thermally isolated from the substrate and contains separate heater and sense resistors. Although promising, these designs have limitations in terms of lack of mechanical stiffness, large thermal mass, and complex fabrication processes.

This paper describes a miniature thermal-isolation design, which achieves a small thermal time constant with low power consumption. The designs illustrated here are compatible with our previously published "epi-seal" wafer-scale encapsulation process [19], [20]; and all its advantages, such as low leak rate, no requirement for a getter, long-term stability [21], and low-cost manufacturing, are maintained. Designs for thermal isolation with various heating methods will be discussed and compared, before presenting the experimental results of the miniature local-thermal-isolation design.

II. Designs for Thermal Isolation

A. Heating Entire Chip for Temperature Control

Thermal isolation of the ovenized device from the surroundings is required to prevent heat loss during temperature control. It is therefore essential to thermally isolate the heater from the ambient but, at the same time, have minimum heat loss between the heater and the resonator. Hence, it is highly desirable to place the heater as close to resonator as possible. An added constraint is to achieve this thermal isolation without modifying the existing fabrication process of the resonator.

A double-ended tuning-fork (DETF)-type resonator, encapsulated within a silicon die (chip), is used (Fig. 1). The chip is attached to the package using an adhesive and wire-bonded to make electrical contacts [Fig. 1(a)]. Heating resistors are placed in the device layer [Fig. 1(b)] in the vicinity of the resonant structure. The DETF is designed for flexural-mode actuation, as shown in Fig. 2. The biased resonator beams are electrostatically actuated by providing an alternating stimulus signal to input electrode. The capacitive transduction between the beams and the input electrodes cause the resonator to vibrate. A resonance occurs when the frequency of the input stimulus signal becomes equal to the natural frequency of the flexural mode of the beam. The output signal is then amplified to measure the resonant frequency.

The power consumption and the thermal time constant can be estimated by using a simple 1-D lumped-parameter thermal model [22], [23]. The expression for conductive thermal resistance is given by

$$R_{\text{th}} = \frac{l}{kA_c}. \tag{1}$$

Thermal capacitance can be evaluated as

$$C_{\text{th}} = \rho V' c_p. \tag{2}$$

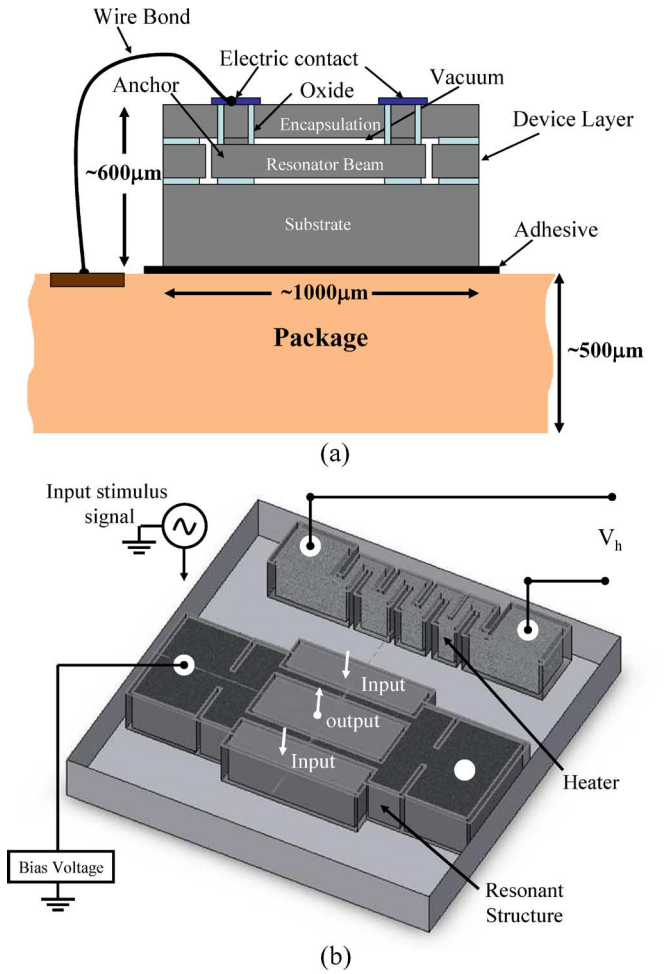

Fig. 1. (a) Schematic of a typical MEMS resonator chip attached to a package with adhesive. (b) Isometric view of the device layer of the chip which contains resonant structure with input–output electrodes and a resistive heater for joule heating. The thickness of the device layer is 20 μm.

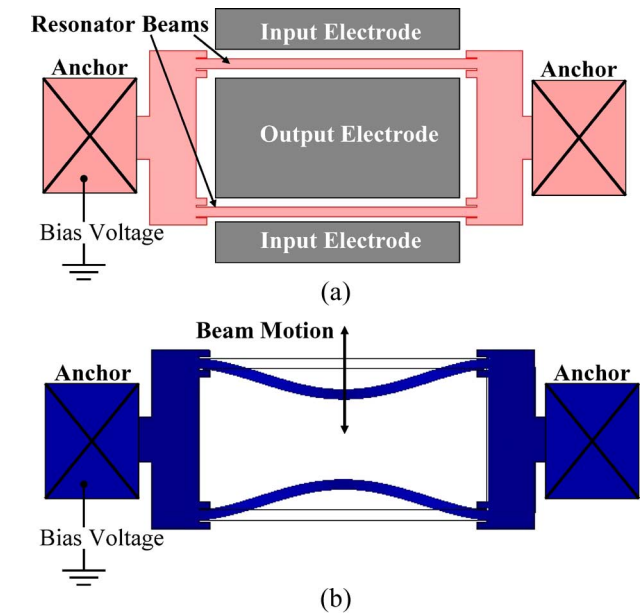

Fig. 2. (a) Top view of DETF-type resonant structure. (b) FEM simulation of flexural-vibration mode of a DETF (exaggerated view).

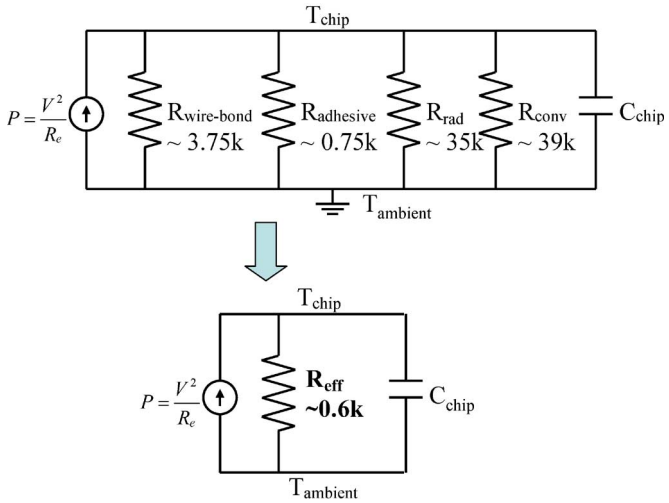

Fig. 3. Thermal equivalent circuit. Package is assumed to be at ambient temperature. Unit of thermal resistances shown above is in Kelvin per watt.

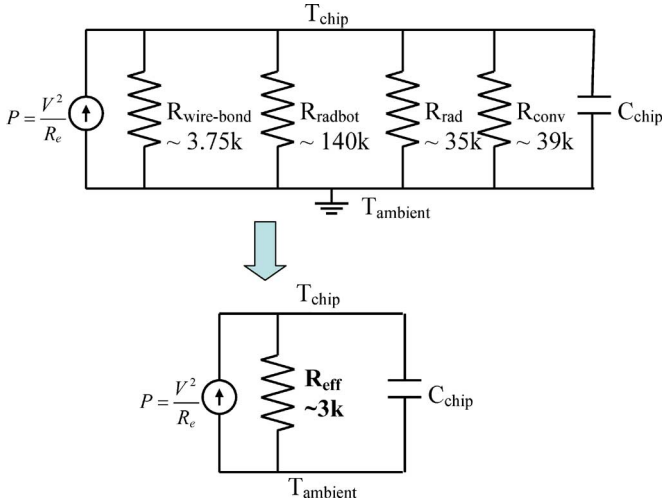

Fig. 4. Thermal equivalent circuit when there is radiative heat loss from the bottom of the chip R_{radbot} in the absence of the adhesive. Unit of thermal resistances shown above is in Kelvin per watt.

Radiative and convective thermal loss can be found by

$$R_{\mathrm{rad}} = \frac{1}{h_{\mathrm{rad}} A_s}$$
$$R_{\mathrm{conv}} = \frac{1}{h_{\mathrm{conv}} A_s} \tag{3}$$

where $h_{\mathrm{rad}} = \varepsilon\sigma(T_s + T_{\mathrm{surr}})(T_s^2 + T_{\mathrm{surr}}^2)$ is the linearized radiation-heat-transfer coefficient [22]. T_s is the surface temperature, and T_{surr} is the surrounding temperature. The h_{conv} is the convective-heat-transfer coefficient. Fig. 3 shows the equivalent thermal-resistance circuit, where P is the input power. Approximate values for the material constants are taken from the literature [24]–[27].

In this design configuration of the MEMS chip, the thermal resistance calculated for the device layer and the chip ($\sim$20 K/W) is very small as compared to that of wire bond and adhesive. It is therefore assumed that the entire chip, including the resonator, is approximately at a constant temperature. It is also assumed that the package acts as a heat sink, and hence, its temperature is the same as the ambient temperature. The total effective thermal isolation R_{eff} is estimated to be approximately 600 K/W.

The power required to achieve a ΔT rise in temperature of the resonator can be found by

$$P = \frac{V^2}{R_e} = \frac{\Delta T}{R_{\mathrm{eff}}}. \tag{4}$$

To obtain ΔT of 125 °C, the input power is approximately 200 mW. The thermal time constant can be estimated by (5) and is approximately 500 ms.

$$\tau = R_{\mathrm{eff}} C_{\mathrm{th}}. \tag{5}$$

One method to improve thermal isolation is to release the chip from the package by removing the adhesive and keep it floating in air, thus reducing the heat loss from substrate to the package. The chip, in this case, is supported from the top by six wire bonds. The equivalent thermal circuit for the released device is shown in Fig. 4, and the total effective thermal isolation is estimated to be approximately 3000 K/W—an improvement by a factor of five.

This method of improving thermal resistance is effective but not robust and may lead to packaging problems. Furthermore, since the heat transfer from the heater to the resonator takes place in the device layer, the device layer gets heated which leads to unwanted heating up of the entire chip because of the lack of thermal isolation between the device layer and the substrate. The thermal mass of a typical resonator chip is approximately 1200 times larger than that of a single DETF, and hence, heating of the entire chip leads to longer thermal time constant and more heat loss resulting in increased input power.

B. Heating Resonator Alone With Local Thermal Isolation

Therefore, it is desired to have an alternative technique to increase the heating efficiency by heating only the resonator and simultaneously providing large thermal isolation between the resonator and its immediate vicinity in the device layer. This calls for a local heat delivery and thermal-isolation mechanism. This can be achieved by designing a resonator coupled with an in-built heater and restricting the heat loss to the ends of the heaters. The in-built heater, in this configuration, serves the dual purpose of heating, as well as thermally isolating, the DETF.

To design a resonator for good thermal isolation, it is necessary to study various heat-loss mechanisms in the structure. The resonator is encapsulated, and the atmosphere inside the encapsulation consists mainly of hydrogen gas at a low pressure of approximately 1 Pa [19]. The three modes of heat transfer considered here are as follows:

1) convection due to hydrogen molecules in the cavity;
2) radiation from the resonator;
3) conduction through the silicon beams of the in-built heater.

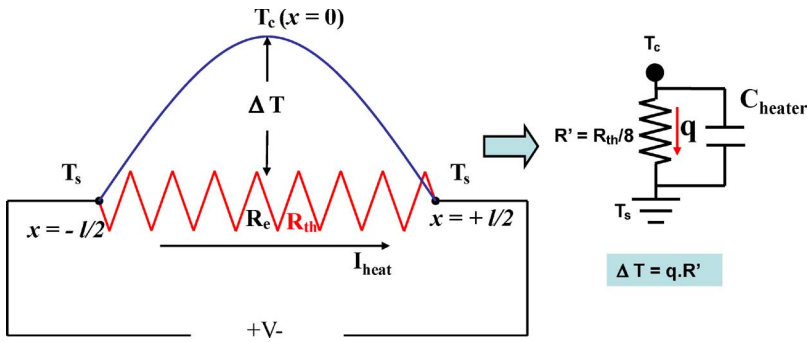

Fig. 5. Temperature profile along the length of a current-carrying resistive heater having thermal resistance of $R_{\rm th}$ and electrical resistance of R_e and its equivalent lumped model.

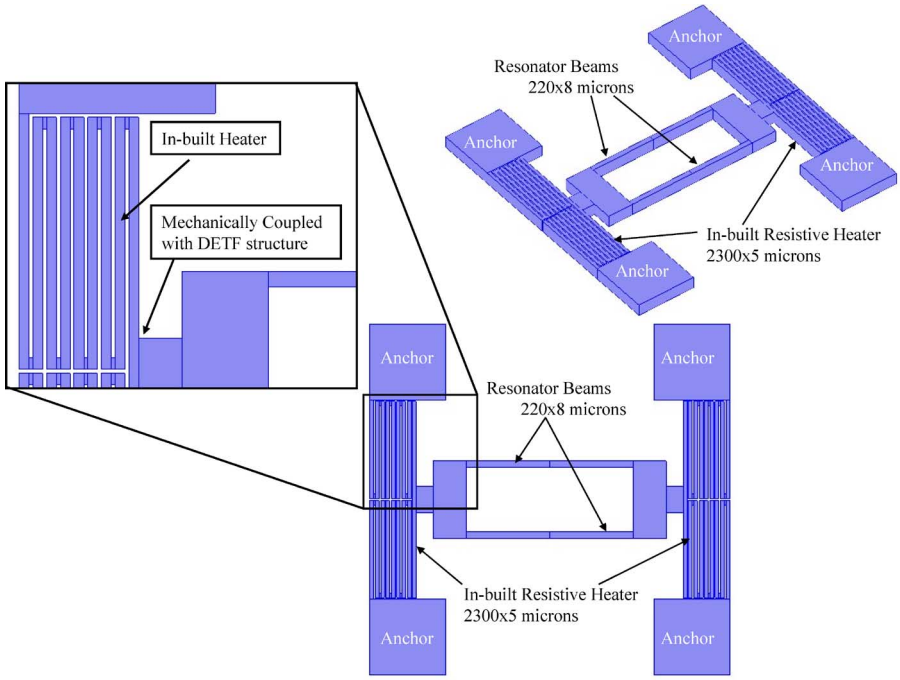

Fig. 6. Resonator design with local thermal isolation. The heater is in-built to the DETF, such that, the resonant structure is attached at the center of the heater. The entire structure is released except at the four anchors.

Convection due to hydrogen molecules can be analyzed by using microscopic-particle-based kinetic theory of heat diffusion [28]. Thermal conductivity of molecular-energy carriers can be evaluated as

$$k_h = \frac{1}{3} C \nu \Lambda \tag{6}$$

where $C = (3/2)k_B n_M$, and $\nu = \sqrt{8k_B T/\pi m}$.

It is assumed that the mean free path Λ is equal to the gap width of the cavity (1.5 μm) because of low pressure. The thermal conductivity due to the hydrogen molecules k_h is estimated to be around 1×10^{-6} W/m/K at room temperature, resulting in an effective thermal resistance of the order of 1×10^7 K/W and, hence, can be assumed that the heat loss due to molecular conduction is negligible as compared to other modes.

The thermal resistance due to radiation for a DETF structure, assumed to be at a maximum heating temperature of 425 K, is estimated to be approximately 1×10^6 K/W. Hence, for simplification, it is also assumed that the heat loss due to radiation is relatively small and can be neglected.

It is, therefore, the conductive heat transfer through the silicon beams which is the dominant heat-loss mechanism in this encapsulated MEMS resonator. If a current-carrying resistive heater of constant cross section is analyzed, the temperature profile along the length of the heater, in the absence of convection and radiation heat loss, is given by (7) [22], [23] and shown in Fig. 5

$$T_x = \left(\frac{q' l^2}{8k}\right)\left(1 - \frac{4x^2}{l^2}\right) + T_s \tag{7}$$

where x varies from $-l/2$ to $+l/2$, and T_s is the end surface temperature of the heater (Fig. 5).

The maximum temperature occurs at the center of the heater (at $x = 0$) and is given by

$$T_c = \left(\frac{q' l^2}{8k}\right) + T_s. \tag{8}$$

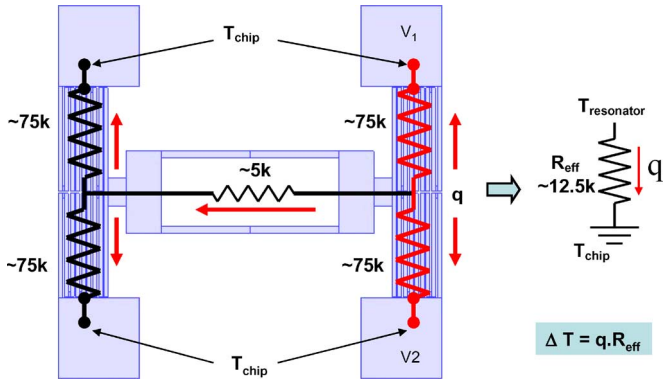

Fig. 7. One-dimensional resistor network to estimate the total effective thermal resistance of the in-built heater. Equation (10) is used for the estimation of effective thermal resistance R_{eff}.

The expression for the rise in temperature at the center of the heater, with respect to its end surface, can be written as

$$\Delta T = T_c - T_s = \frac{q' l^2}{8k} = \left(\frac{V^2}{R_e}\right)\left(\frac{R_{\text{th}}}{8}\right) = qR' \qquad (9)$$

where $q' = q/lA = ((V^2/R_e)/lA)$.

From (9), we can establish an equivalence between a current-carrying beam having thermal resistance of R_{th} and heat generation of q with a lumped model having thermal resistance of R' and heat flow of q for the same rise in temperature, where R' is eight times smaller than R_{th}. This suggests that the heating efficiency can be maximized if the resonator is attached at the center of the heater and that, in order to achieve the maximum temperature rise at the center of the heater for a given input power, the thermal resistance of the heater should be as large as possible.

However, the micro-ovenized resonator design is suspended from both ends by in-built resistors (Fig. 6), so the expression for the temperature of the resonator due to heating power applied to one end of the resonator must take into account the heat loss through the other end of the resonator. Using the equivalent thermal resistance from (9), we can estimate the resonator temperature by considering the second resistor in parallel with the heater resistor (Fig. 7). In this case, an approximate expression for the rise in temperature at the center of the heater, with respect to its end surface, can be written as

$$\Delta T \sim \left(\frac{V^2}{R_e}\right)\left(\frac{1}{\frac{1}{(R_{\text{th}}/8)} + \frac{1}{(R_{\text{th}}/4)}}\right) = \left(\frac{V^2}{R_e}\right)\left(\frac{R_{\text{th}}}{12}\right) = qR_{\text{eff}}. \qquad (10)$$

From (10), for a resonator with a heating resistor with internal heat generation of q at one end and an insulating resistor with no heat generation at the other end, both having thermal resistance of R_{th}, we can establish an equivalent lumped-element model with a thermal resistance of R_{eff} and heat flow of q for the same rise in temperature, where R_{eff} is 12 times smaller than R_{th}. This relationship allows us to easily predict the resonator temperature for a given heating power, although the prediction is not exact because the temperature distribution on the heater is modified by the heat flow across the resonator.

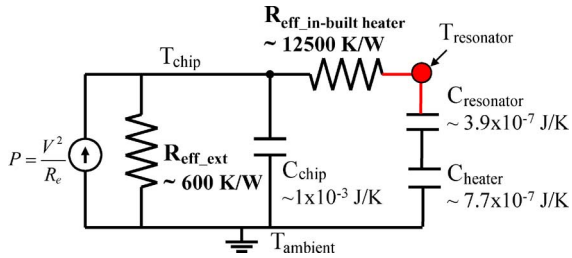

Fig. 8. Equivalent thermal circuit schematic for the resonator with in-built heater.

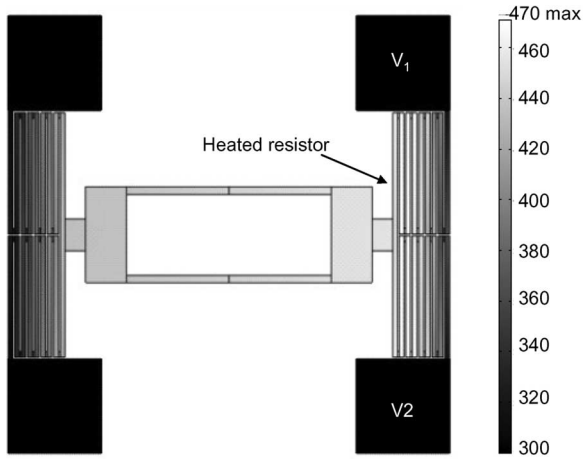

Fig. 9. Finite-element simulation of the thermally isolated DETF resonator showing the temperature distribution in Kelvin for a heating voltage of 6 V, which corresponds to 14 mW of heating power.

TABLE I
POWER CONSUMPTION AND TIME-CONSTANT COMPARISON

Design	Power required for 125 °C temperature increase	Estimated Thermal Time Constant
Bonded chip[1]	~ 200 mW	~ 500 ms
Suspended chip	~ 42 mW	~ 3000 ms
In-built heater	~ 12 mW	~15 ms

[1]Conventional Design

Finite-element simulations (Fig. 9) and measurements indicate that (10) overestimates the resonator temperature by about 20%.

The layout of the thermally isolated DETF with two in-built heaters is shown in Figs. 6 and 7. The cross section of each heater beam is 5 by 20 μm, and its total length is approximately 2300 μm. The resonator is attached at the center of the heater for maximum heating. The entire structure is released except at the four anchors which act as mechanical supports at the bottom and provide electrical contacts at the top. The anchors are electrically insulated by silicon dioxide [see Fig. 1(a)]. The thermal resistance of the in-built heater R_{th} is approximately 150 000 K/W. Fig. 7 shows an equivalent lumped-capacitance model of the DETF with in-built heater. The effective thermal resistance R_{eff} of the micro-ovenized structure is calculated using (10) and is evaluated to be approximately 12 500 K/W, which is significantly larger than nonisolated designs.

The thermal isolation of the resonator also leads to a reduced thermal time constant, because the effective thermal mass comprises only the mass of the DETF and the in-built resistors,

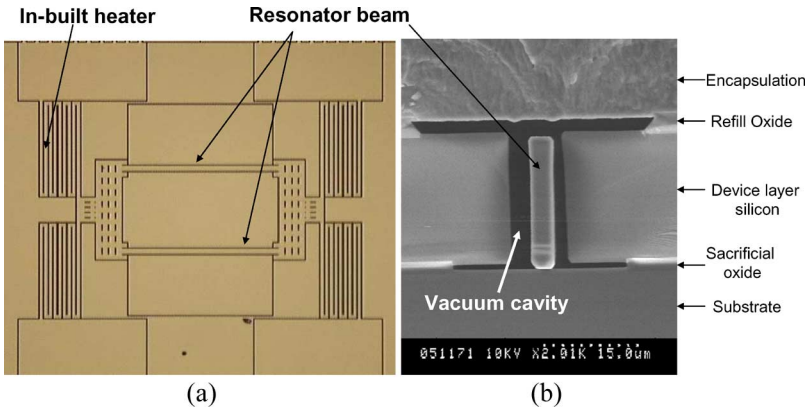

Fig. 10. (a) Optical image of the top view of the fabricated device before the deposition of the encapsulation layer. (b) SEM cross section of a resonator beam after the deposition of the encapsulation layer.

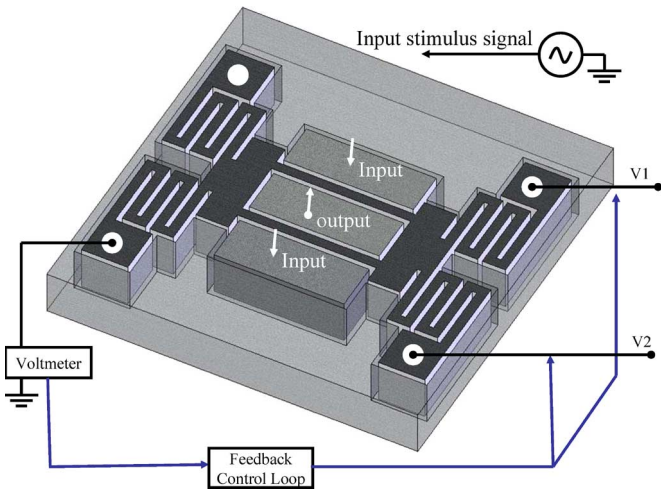

Fig. 11. Isometric view of device layer schematic showing the DETF with the in-built heater. A stimulus signal is applied to the input electrode. Heating voltages V_1 and V_2 are controlled using a feedback control loop to maintain a constant bias for the resonator.

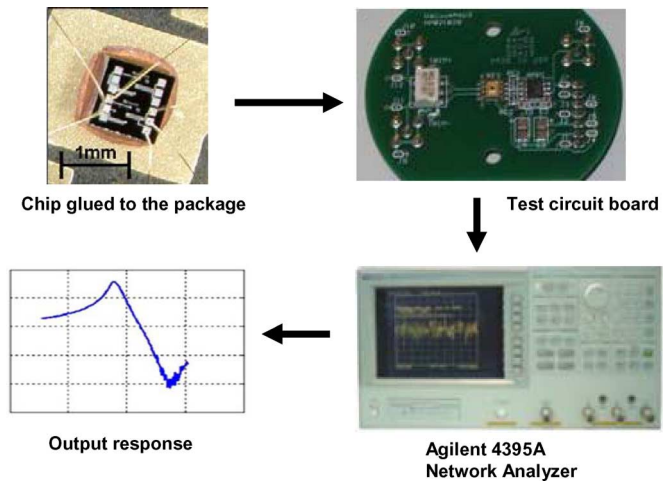

Fig. 12. Schematic of the test setup for frequency measurement.

as opposed to the entire silicon die described in Section II-A. This means that there will be rapid heating and cooling of the resonator over and above the slower thermal response of the chip. A 1-D equivalent thermal-circuit model of the in-built heater is shown in Fig. 8. As with temperature, the thermal time constant of the resonator cannot be calculated precisely by a simple lumped-element model because of the complex temperature profile through the device, but we can make an estimate using the effective resistance of the heaters and the total thermal capacitance of the heaters and the resonator, as shown in

$$\tau = R_{\text{eff}}(C_{\text{resonator}} + C_{\text{heaters}}) \tag{11}$$

$$\tau_{\text{chip}} \approx R_{\text{eff\_ext}} C_{\text{chip}}. \tag{12}$$

For the thermally isolated DETF, τ is estimated to be approximately 15 ms. The actual dynamic behavior of the device is characterized by multiple time constants from the nonheated resistor, the silicon die, and the resonator. Finite-element simulations indicate that the temperature change of the resonator itself may be up to 50% slower than the heaters.

A finite-element simulation was done to examine the temperature distribution along the length of the in-built heater and the DETF, as shown in Fig. 9. From the simulation, a power consumption of approximately 12 mW was required for a temperature increase of 125 °C. The time constant and heating power consumption of the three designs are compared in Table I. Clearly, the in-built heater can be very effective, both in terms of reducing power consumption and dynamic thermal response.

III. Fabrication

One of the biggest advantages of this technique is with respect to fabrication. A CMOS compatible "epi-seal" encapsulation process [19], [20] is used to fabricate this device. The structure of the fabricated device is shown in Fig. 1(a). The device layer is insulated from the encapsulation layer by a thin sacrificial oxide, and openings for electrical contacts are made through the encapsulation layer over the anchors. Since the in-built heaters are in the device layer with the resonator, no changes to the fabrication process are required to create the thermally isolated DETF. This process ensures a vacuum inside the encapsulation with a pressure of < 1 Pa. Long term

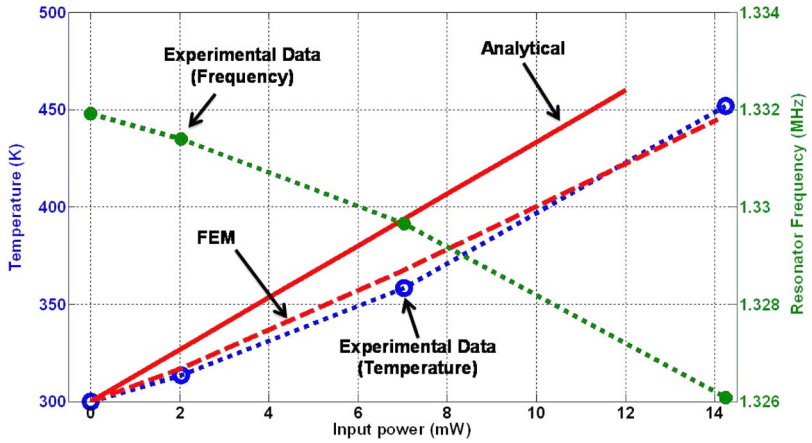

Fig. 13. Variation of resonator frequency due to joule heating of the in-built heater. The decrease in frequency (right y-axis) corresponds to a temperature rise (left y-axis) with increasing input power. Experimental results are compared with theoretical estimates. The analytical expression (10) estimates the temperature at the center of the in-built heater, while the FEM results are for the temperature at the center of the resonator.

($\sim$1 year) stability of this vacuum condition has also been verified [21]. An optical image and a SEM cross section of encapsulated MEMS resonator with in-built heater is shown in Fig. 10.

IV. Experimental Results

Resonators with 1.3-MHz frequency and a mechanical Q of approximately 10^4 were used for the experiment. Since silicon resonator frequency varies nearly linearly with temperature [24], [29], frequency was used as a measure of temperature for this work. However, resonator frequency is also sensitive to bias voltage and axial strain.

The bias voltage induces capacitive nonlinearity, which causes the effective stiffness of the resonator beam to decrease [29], reducing the resonator frequency. It is necessary to ensure that the bias voltage is not affected by the heating current. Fig. 11 shows the device layer schematic with circuit diagram of the resonator having in-built heater. Voltages V_1 and V_2 are applied, such that the potential difference between them acts as a joule heating voltage V_h across the in-built heater

$$V_1 = V_b + \frac{V_h}{2}$$
$$V_2 = V_b - \frac{V_h}{2} \tag{13}$$

where V_b is the effective bias voltage. Ideally, the resonator should see a constant bias voltage, because the portions of the in-built heaters, before and after the resonator, are nominally identical, but fabrication uncertainties result in asymmetry of the heaters that cause the bias voltage to change with the heating voltage. To remove the effect of this change in bias, a feedback-control loop was implemented to maintain a constant bias voltage on the resonator irrespective of the variable heating voltage. The bias-control circuit had a compliance of 1.0 mV, which is equivalent to a < 0.1 ppm change in frequency. A schematic of the experimental test setup is shown in Fig. 12, and the results of the measurement are shown in Fig. 13.

Stress due to differential thermal expansion of the device layer, the chip, and the package can create compressive axial strain on the DETF, leading to a shift in frequency. The natural frequency of the resonator beam in the presence of compressive axial force can be found using the following expression [30]:

$$f = \frac{(4.73)^2}{2\pi l^2}\left(1 + \frac{Pl^2}{EI\pi^2}\right)^{\frac{1}{2}}\left(\frac{EI}{m}\right)^{\frac{1}{2}}. \tag{14}$$

The stiffness of the in-built heater is approximately 10 000$\times$ smaller than the resonator beams, and the resulting frequency error due to differential thermal expansion of the heater is estimated to be within 0.5% of the total change in frequency due to a temperature increase of 150 °C. Since the error is not large and we are interested in the approximate estimation of the power consumption, we ignore this error. The resonator was calibrated in a thermal chamber by measuring its frequency at different ambient temperatures with no power applied to the in-built heaters. The measured temperature coefficient of frequency was found to be nearly linear and equal to -29 ppm/°C, which is approximately the same as that of a stress-free single-anchor silicon resonator [24], [31].

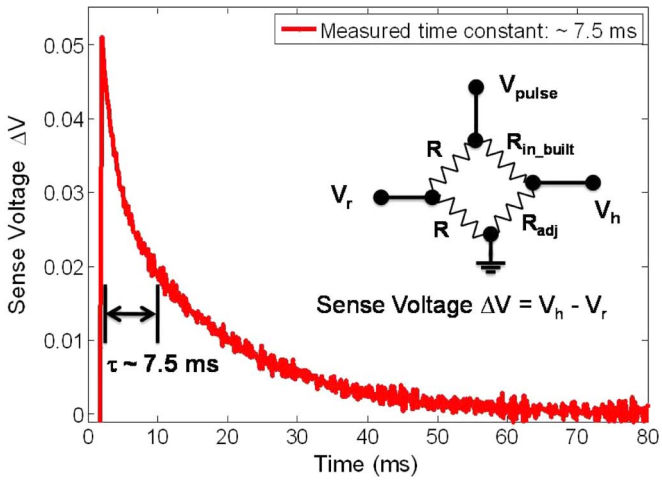

Fig. 14. Dynamic thermal response of the micro-ovenized resonator. (Inset) The in-built heater formed one leg of a wheatstone bridge. The measured voltage output from the bridge represents the change in heater resistance as the heater cools down following a heating pulse.

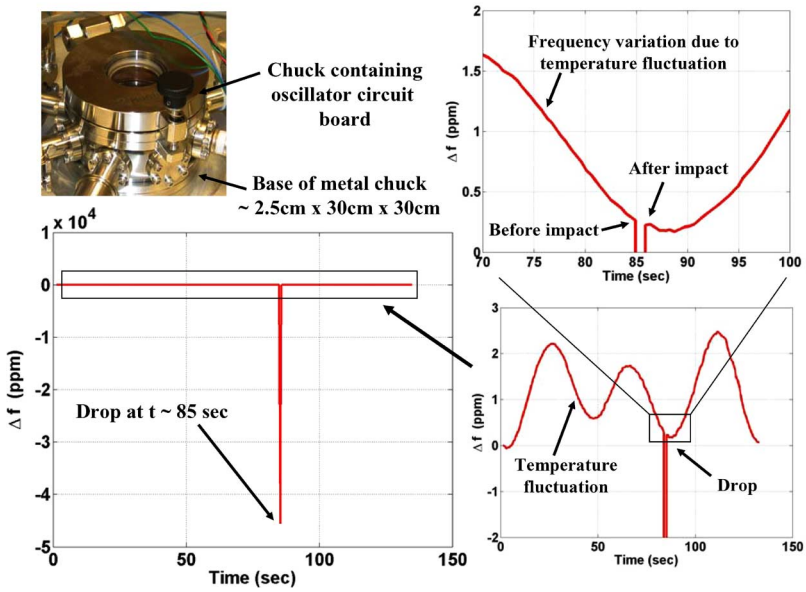

Fig. 15. Drop test resulted in a temporary change in frequency at the time of drop.

It is also necessary to check the influence of the in-built heater suspension on the mechanical quality factor (Q) of the resonator. Since the heater suspension is on both sides of the DETF, there is a linear temperature gradient across the length of the resonator beam. This gradient in temperature affects the Q. It has been shown [32] that the Q for a resonator with a linear temperature gradient and average temperature T_A will be slightly higher than the Q of a resonator with no temperature gradient and uniform temperature T_A. However, the temperature gradient has a minimal effect on the frequency–temperature calibration of the resonator.

A. Power Consumption

The DETF was heated using the in-built heater, and its frequency was measured as a function of input power. As shown in Fig. 13, the frequency decreases with the increase in input power as the temperature rises. The temperature rise was evaluated using the calibration data of frequency versus oven temperature. It has been observed that there is a rise in temperature of approximately 125 °C with total power consumption of around 12 mW. The experimental output is observed to be slightly nonlinear as compared to the simulation results. This can be attributed to the fact that the material properties, including thermal conductivity and electrical resistivity of silicon, vary with temperature but were considered constant for the calculation.

B. Thermal Time Constant

The thermal time constant of the micro-ovenized resonator is an important parameter for temperature control. The thermal response was evaluated using a transient electrical-resistance measurement. A voltage pulse was applied to the heater, which caused its resistance to increase as it heated up. After the pulse ended, the heater resistance decreased as it cooled. A wheatstone bridge was used to measure the change in heater resistance during this cycle (Fig. 14). For the measurement, a heating pulse of 4.5 V was used, and the voltage was maintained at 0.5 V during the cooling period in order to observe the change in voltage during cooling.

The measured time constants of several resonators varied between 7 and 10 ms. A typical measurement is shown in Fig. 14. We expect the measurement to understate the time constant, because the measurement indicates the average temperature of the heater, not the temperature of the resonator itself. It is to be noted that the thermal capacitance of the DETF is approximately equal to that of an in-built heater, and so, there is potential in reducing the thermal time constant in future designs by reducing the thermal mass of the resonator itself.

C. Impact Resistance of Mechanical Suspension

The thermal resistance of the resistive heater directly depends on the length of the beam and is inversely proportional to its cross-sectional area. Design of a large thermal resistance is limited by the reduction of mechanical stiffness of the structure. However, miniaturization allows a stiffer design of the heater having relatively higher thermal resistance. To investigate the stiffness of the thermally isolated DETF structure, a drop test was carried out. The chip was soldered to an oscillator circuit board, which was rigidly bolted to a heating chuck (Fig. 15) maintained at a constant temperature of 70 °C. The chuck was dropped from a height of 1.0 cm onto a rigid platform, and the response of the resonator frequency was measured, as shown in Fig. 15. At the time of impact, the oscillator frequency changed by approximately −45 000 ppm. The resonator immediately returned to normal operation. The change in frequency before and after the impact is within the noise of the frequency fluctuation of the uncompensated resonator due to small variation in the chuck temperature, as shown in Fig. 15. Furthermore, the resonators survived the 5000-rpm rotation (up to ∼1400 g of acceleration) during the photoresist spin-coating steps of the fabrication process. The spin duration was approximately 1 min and was repeated six to eight times during the fabrication.

V. Conclusion

An efficient heat delivery and thermal-isolation mechanism for a MEMS resonator has been demonstrated. The in-built heater-based thermal-isolation technique serves a dual purpose of localized heating and local thermal isolation, thereby providing maximum heating with minimized input power. At the same time, the device has a small thermal time constant and high impact resistance because of its miniature design. Compared to the commercially used quartz crystals (1–10 W and around 30 min warm-up time), this paper has demonstrated orders-of-magnitude improvement in power dissipation and dynamic thermal response with a potential for further improvement. Furthermore, this method is simple enough to implement it into any existing MEMS fabrication process. The described design of microoven is highly suitable for temperature stabilization of microresonators and for very precise control of frequency (< 1.0 ppm) over a large temperature span. Future work will focus on designing thermal-isolation structures with a single point of attachment to the resonator, which will improve performance by eliminating temperature gradients across the resonator and by reducing power consumption and thermal capacitance.

References

[1] C. T.-C. Nguyen, "MEMS technology for timing and frequency control," *IEEE Trans. Ultrason., Ferroelectr., Freq. Control*, vol. 54, no. 2, pp. 251–270, Feb. 2007.

[2] V. Kaajakari, J. Kiihamaki, A. Oja, S. Pietikainen, V. Kokkala, and H. Kuisma, "Stability of wafer level vacuum encapsulated single-crystal silicon resonators," *Sens. Actuators A, Phys.*, vol. 130/131, pp. 42–47, Aug. 2006.

[3] C. T.-C. Nguyen and R. T. Howe, "An integrated CMOS micromechanical resonator high-Q oscillator," *IEEE J. Solid-State Circuits*, vol. 34, no. 4, pp. 440–455, Apr. 1999.

[4] D. Sparks, S. Massoud-Ansari, and N. Najafi, "Chip-level vacuum packaging of micromachines using nanogetters," *IEEE Trans. Adv. Packag.*, vol. 26, no. 3, pp. 277–282, Aug. 2003.

[5] W.-T. Hsu and C. T.-C. Nguyen, "Stiffness-compensated temperature-insensitive micromechanical resonators," in *Proc. IEEE MEMS*, 2002, pp. 731–734.

[6] E. P. Quevy and R. T. Howe, "Redundant MEMS resonators for precise reference oscillators," in *Proc. IEEE Radio Freq. Integr. Circuits Symp.*, 2005, pp. 113–116.

[7] M. A. Hopcroft, M. Agarwal, K. K. Park, B. Kim, C. M. Jha, R. N. Candler, G. Yama, B. Murmann, and T. W. Kenny, "Temperature compensation of a MEMS resonator using quality factor as a thermometer," in *Proc. 19th IEEE Int. Conf. MEMS*, Jan. 2006, pp. 222–225.

[8] J. R. Vig, "Temperature-insensitive dual-mode resonant sensors—A review," *IEEE Sensors J.*, vol. 1, no. 1, pp. 62–68, Jun. 2001.

[9] R. L. Filler and J. R. Vig, "Resonators for the microcomputer compensated crystal oscillator," in *Proc. 43rd Annu. Freq. Control Symp.*, 1989, pp. 8–15.

[10] J. R. Vig, "Temperature stable crystal oscillator," *IEEE Trans. Ultrason., Ferroelectr., Freq. Control*, vol. 42, no. 4, pp. 797–799, Jul. 1995.

[11] A. Ballato and J. R. Vig, "Static and dynamic frequency-temperature behavior of singly and doubly rotated, oven-controlled quartz resonators," in *Proc. 32nd FCS*, 1978, pp. 180–188. AD-A955 718.

[12] I. Balaz and M. Minarik, "Towards an OCXO with infrared heater," in *Proc. IEEE Int. FCS*, 1996, pp. 674–680.

[13] M. Vaish, "A high precision quartz oscillator with performance comparable to rubidium oscillators in many respects," in *Proc. IEEE Int. FCS*, 1996, pp. 752–760.

[14] Vectron International, *C4550 OCXO*. [Online]. Available: http://www.vectron.com

[15] M. E. Frerking, *Crystal Oscillator Design and Temperature Compensation*. New York: Van Nostrand, 1978.

[16] C. T.-C. Nguyen and R. Howe, "Microresonator frequency control and stabilization using an integrated micro oven," in *Proc. Transducers*, Yokohama, Japan, 1993, pp. 1040–1043.

[17] C. T.-C. Nguyen, "Micromechanical resonators for oscillators and filters," in *Proc. IEEE Ultrason. Symp.*, 1995, vol. 1, pp. 489–499.

[18] M. A. Huff, S. D. Senturia, and R. T. Howe, "Thermally isolated microstructure suitable for gas sensing applications," in *Tech. Dig. IEEE Solid-State Sens., Actuator Workshop*, Hilton Head, SC, Jun. 6–9, 1988, pp. 47–50.

[19] R. N. Candler, M. A. Hopcroft, B. Kim, W. T. Park, R. Melamud, M. Agarwal, G. Yama, A. Partridge, M. Lutz, and T. W. Kenny, "Long-term and accelerated life testing of a novel single-wafer vacuum encapsulation for MEMS resonators," *J. Microelectromech. Syst.*, vol. 15, no. 6, pp. 1446–1456, Dec. 2006.

[20] R. N. Candler, W.-T. Park, H. Li, G. Yama, A. Partridge, M. Lutz, and T. W. Kenny, "Single wafer encapsulation of MEMS devices," *IEEE Trans. Adv. Packag.*, vol. 26, no. 3, pp. 227–232, Aug. 2003.

[21] B. Kim, R. N. Candler, M. A. Hofcroft, M. Agarwal, W.-T. Park, and T. W. Kenny, "Frequency stability of wafer-scale film encapsulated silicon based MEMS resonators," *Sens. Actuators A, Phys.*, vol. 136, no. 1, pp. 125–131, May 2007.

[22] F. P. Incropera and D. P. Dewitt, *Fundamentals of Heat and Mass Transfer*, 5th ed. New York: Wiley, 2002.

[23] M. N. Ozisik, *Heat Conduction*, 2nd ed. New York: Wiley, 1993.

[24] C. Bourgeois, E. Steinsland, N. Blanc, and N. F. de Rooij, "Design of resonators for the determination of the temperature coefficients of elastic constants of monocrystalline silicon," in *Proc. IEEE Int. Freq. Control Symp.*, 1997, pp. 791–799.

[25] J. D. Plummer, M. Deal, and P. B. Griffin, *Silicon VLSI Technology: Fundamentals, Practice, and Modeling*. Englewood Cliffs, NJ: Prentice-Hall, 2000.

[26] A. D. McConnell, U. Srinivasan, and K. E. Goodson, "Thermal conductivity of doped polysilicon layers," *J. Microelectromech. Syst.*, vol. 10, no. 3, pp. 360–369, Sep. 2001.

[27] M. Asheghi, K. Kurabayashi, R. Kasnavi, and K. E. Goodson, "Thermal conduction in doped single crystal silicon films," *J. Appl. Phys.*, vol. 91, no. 8, pp. 5079–5088, Apr. 2002.

[28] W. G. Vincenti and C. H. Kruger, Jr., *Introduction to Physical Gas Dynamics*. New York: Wiley, 1975.

[29] V. Kaajakari, T. Mattila, A. Oja, and H. Seppa, "Nonlinear limits for single-crystal silicon microresonators," *J. Microelectromech. Syst.*, vol. 13, no. 5, pp. 715–724, Oct. 2004.

[30] R. D. Blevins, *Formulas for Natural Frequency and Mode Shape*. Malabar, FL: Krieger, 2000.

[31] R. Melamud, M. A. Hopcroft, C. M. Jha, B. Kim, S. A. Chandorkar, R. N. Candler, and T. W. Kenny, "Effects of stress on the temperature coefficient of frequency in double clamped resonators," in *Proc. Solid-State Sens., Actuators, Microsyst.*, 2005, vol. 1, pp. 392–395.

[32] S. A. Chandorkar, H. Mehta, M. Agarwal, M. A. Hopcroft, C. M. Jha, R. N. Candler, G. Yama, G. Bahl, B. Kim, R. Melamud, K. E. Goodson, and T. W. Kenny, "Non-isothermal micromechanical resonators," in *Proc. MEMS*, Kobe, Japan, 2007.

Chandra Mohan Jha received the B.E. degree in mechanical engineering from the Birla Institute of Technology, Mesra, India, in 1996 and the M.S. degree in mechanical engineering from Stanford University, Stanford, CA, in 2006. He is currently working toward the Ph.D. degree in the Department of Mechanical Engineering and the Department of Electrical Engineering, Stanford University.

From 1996 to 1997, he was with LML Ltd., India, as an Engineer. From 1997 to 2004, he was with Bhabha Atomic Research Centre as a Scientific Officer, working on design and development of mechanical systems for harsh environments. His current research is focused on the design and optimization of micro-oven-based MEMS resonators for low power and high-temperature stability.

Mr. Jha is a Student Member of the American Society of Mechanical Engineers (ASME).

Matthew A. Hopcroft received the B.Sc. degree in computer engineering from the George Washington University, Washington, D.C., in 1998, the M.Phil. degree from Cambridge University, Cambridge, England, in 2002, and the Ph.D. degree in mechanical engineering from Stanford University, Stanford, CA, in 2007.

He is currently a Research Specialist with the Berkeley Micromechanical Analysis and Design Group and the Berkeley Sensor and Actuator Center, University of California, Berkeley. His research interests include MEMS material property measurements, microscale and portable power systems, and micromechanical resonators.

Saurabh A. Chandorkar received the B.Tech. degree in mechanical engineering from the Indian Institute of Technology, Mumbai, India, in 2003 and the M.S. degree in mechanical engineering from Stanford University, Stanford, CA, in 2005. He is currently working toward the Ph.D. degree at Stanford University.

His current research interests include the study of energy loss mechanisms, namely, thermoelastic dissipation, Akhieser effect loss and clamping loss, and micromechanical resonators.

James C. Salvia (S'03) received the B.S. degree in electrical and computer engineering from Carnegie Mellon University (CMU), Pittsburgh, PA, in 2005. He is currently working toward the M.S. and Ph.D. degrees in electrical engineering at Stanford University, Stanford, CA.

He was a Research Assistant with CMU, where he developed on-chip magnetic inductors for high-frequency applications. He is currently with the Microstructures and Sensors Laboratory, Department of Mechanical Engineering and the Department of Electrical Engineering, Stanford University, working on circuit development for the stabilization and control of microresonator-based oscillators.

Manu Agarwal (S'01–M'06) received the B.Tech. degree in electrical engineering from the Indian Institute of Technology, Kanpur, India, in 2003 and the M.S. and Ph.D. degrees in electrical engineering, with a doctoral thesis on modeling nonlinearities in electrostatically actuated MEMS resonators and study of their impact on phase noise, from Stanford University, Stanford, CA, in 2005 and 2007, respectively.

He was an Intern with the Technical University of Ilmenau, Ilmenau, Germany, and the Ecole Polytechnique Fédérale de Lausanne, Lausanne, Switzerland. He was an Intern with Agilent Labs, Palo Alto, CA, working on characterizing dipole surface drive MEMS actuators. He is currently with Netlogic Microsystems, Mountain View, CA, working as a Mixed-Signal Circuit Design Engineer. He is the author or coauthor of more than 30 technical publications. He is the holder of one U.S. patent.

Rob N. Candler (S'98–M'00) received the B.S. degree in electrical engineering from Auburn University, Auburn, AL, in 2000 and the M.S. and Ph.D. degrees in electrical engineering from Stanford University, as a National Defense Science and Engineering Graduate Fellow, in 2002 and 2006, respectively.

He was a Consulting Assistant Professor with the Department of Electrical Engineering and the Department of Mechanical Engineering, Stanford University. He is currently a Senior Research Engineer with Bosch Research and Technology Center, Palo Alto, CA, working on MEMS-based sensors for automotive and commercial markets. He also directs Bosch's involvement in the DARPA Science and Technology Fundamentals program. His research interests include RF MEMS, wafer-scale sensor packaging, and sensor reliability.

Renata Melamud received the B.S. degree in mechanical engineering from Carnegie Mellon University, Pittsburgh, PA, in 2003 and the M.S. degree in mechanical engineering from Stanford University, Stanford, CA, in 2006. She is currently working toward the Ph.D. degree in the Department of Mechanical Engineering and the Department of Electrical Engineering, Stanford University, wherein she is supported by the Gabilan Stanford Graduate Fellowship for her research on passive compensation techniques to reduce the temperature dependence of frequency in silicon resonators.

Bongsang Kim received the B.S. degree in mechanical design and production engineering from Seoul National University, Seoul, Korea, and the M.S. and Ph.D. degrees in mechanical engineering from Stanford University, Stanford, CA, in 2004 and 2007, respectively.

From 1998 to 2001, he was with Hyundai Mobis as a Mechanical Engineer. He was an Intern with Agilent Labs, Palo Alto, CA, in 2005, working on the development of nanostepper for AFM application. He is currently a Postdoctoral Researcher with the University of California, Berkeley. His research interests include RF MEMS, reliability of MEMS structures, MEMS packaging, material diffusion, and energy loss and stability of micromechanical resonators.

Dr. Kim received the Best Student Poster Presentation Award at the IEEE Frequency Control Symposium 2007.

Thomas W. Kenny received the B.S. degree in physics from the University of Minnesota, Minneapolis, in 1983 and the M.S. and Ph.D. degrees in physics from the University of California, Berkeley, in 1987 and 1989, respectively.

From 1989 to 1993, he was with NASA Jet Propulsion Laboratory, working on the development of electron-tunneling high-resolution microsensors. Since 1994, he has been with the Department of Mechanical Engineering and the Department of Electrical Engineering, Stanford University, Stanford, CA, where he directs MEMS-based research in a variety of areas including resonators, wafer-scale packaging, cantilever beam force sensors, microfluidics, and novel fabrication techniques for micromechanical structures. He is a Founder and Chief Technical Officer of Cooligy, a microfluidics chip cooling components manufacturer and Founder and Board Member of SiTime, a developer of CMOS timing references using MEMS resonators. He is currently a Stanford Bosch Faculty Development Scholar and is serving as a Program Manager with the Microsystems Technology Office, DARPA. He is the author or coauthor of more than 200 scientific papers. He is the holder of 40 patents.